Effects of Concentration, Temperature and Hydrostatic Pressure on the Local Lattice Structure of Ni^{2+} Doped $Zn(BF_4)_2 \cdot 6H_2O$ Crystal

Ming-Liang Gao[a], Xiao-Yu Kuang[a,b], Hui-Fang Li[a], and Huai-Qian Wang[a]

[a] Institute of Atomic and Molecular Physics, Sichuan University, Chengdu 610065, China
[b] International Centre for Materials Physics, Academia Sinica, Shenyang 110016, China

Reprint requests to X.-Y. K.; E-mail: scu_kuang@163.com

Z. Naturforsch. **64a,** 511 – 517 (2009); received October 9, 2008 / revised December 29, 2008

A theoretical method for studying the inter-relationship between electronic and molecular structure is presented by means of complete energy matrices. As an application, the effects of temperature, concentration and hydrostatic pressure on the local structures of Ni^{2+} doped $Zn(BF_4)_2 \cdot 6H_2O$ crystal have been studied. Our results show that the local lattice structures of $[Ni(H_2O)_6]^{2+}$ coordination complex have expansion distortions as the temperature rises. Meanwhile, we find that the local structure parameter θ becomes smaller with the increasing concentration of Ni^{2+} ions doped in $Zn(BF_4)_2 \cdot 6H_2O$ crystal. Furthermore, the pressure dependence of θ and anisotropic g-factors are discussed and the relationship between zero-field splitting parameter D and Δg is determined.

Key words: Local Structure; $Zn(BF_4)_2 \cdot 6H_2O$:Ni^{2+} System; Complete Energy Matrices.

1. Introduction

With the rapid development of material science, solid material crystals doped with transition metal ions have drawn a great deal of attention in recent years [1 – 5]. This can be attributed to the fact that crystals with transition metal ions usually have special behaviours [6 – 9] which are closely related to the structure distortions. Accordingly, studying the local structures around the impurities is crucial to get a better insight into the interaction between impurity ions and host crystals and is central to realize the microscopic origin of crystal properties.

Experimentally, many methods are used to investigate the local structure of the doped systems, such as the electron nuclear double resonance (ENDOR) [10 – 12], the extended X-ray absorption fine structure (EXAFS) [13 – 15] and the electron paramagnetic resonance (EPR) [16 – 18]. Among them, the EPR method is considered as a powerful tool to study the microstructures and the local distortions around the impurity ions in the crystals. The reason is that the EPR spectra are sensitive to the distortion of the local structures of the transition metal ions [19, 20]. The EPR spectra of Ni^{2+} ions in $Zn(BF_4)_2 \cdot 6H_2O$:Ni^{2+}system have been measured by many researchers [21 – 24]. For instance, Sano et al. have studied the temperature and concentration dependence of the EPR spectra of $Zn(BF_4)_2 \cdot 6H_2O$:Ni^{2+}system [21]. Krygin et al. have dealt with the pressure dependence of the EPR parameters of Ni^{2+} ions doped in $Zn(BF_4)_2 \cdot 6H_2O$ crystal [22]. Their experimental results give important information about the ground state of the transition metal Ni^{2+} ions and form a useful starting point for understanding the inter-relationship between electronic and molecular structure of Ni^{2+} ions in the $[Ni(H_2O)_6]^{2+}$ coordination complex. So far, however, few systematical studies on the local structure parameters of $[Ni(H_2O)_6]^{2+}$coordination complex at different concentrations, temperatures and pressures have been reported. Recently, Feng et al. have studied the effects of the temperature and pressure on the zero-field splitting (ZFS) and got the local structure parameters $\theta = 54.80^\circ$ at 77 K and $\theta = 54.95^\circ$ at 293 K by the complete energy matrices using a Matlab 6.5 computer program [25], but their method is based on the strong-field basis function and the local structure parameters under different concentrations have not been investigated. In the present work, the 45×45 complete energy matrices have been constructed based on the weak-field basis function in terms of the Slater's method. The relations between the local structure and concentration, temperature and pressure are discussed systematically.

2. Theoretical Analysis

2.1. The Complete Energy Matrices for a d^8 Configuration Ion in a Trigonal Ligand Field

For the paramagnetic Ni^{2+} ion in a trigonal symmetry field, the complete set of basis function includes 45 basic Slater determinants such as $|2^+,2^-|$, $|2^+,1^-|,\ldots,|-2^+,-2^-|$. Then, the wave functions $|L,S,M_l,M_s\rangle_i$ of d^8 configuration in the LS-coupling scheme can be gotten based on the following expression

$$|L,S,M_l,M_s\rangle_i = \sum_j C_j \Phi_j, \tag{1}$$

where C_j is the Clebsch-Gordon coefficient and Φ_j is one of the 45 basic Slater determinants.

The perturbation Hamiltonian for a d^8 configuration ion in a trigonal ligand-field can be expressed as [25]

$$\begin{aligned}\hat{H} &= \hat{H}_{ee} + \hat{H}_{SO} + \hat{H}_{LF} + \hat{H}_{Zeeman} \\ &= \sum_{i<j} \frac{e^2}{r_{i,j}} + \zeta \sum_i l_i s_i + \sum_i V_i \\ &\quad + \sum_i \mu_B (k\vec{l}_i + g_e \vec{s}_i) \cdot \vec{H},\end{aligned} \tag{2}$$

where the first term is the electron-electron interaction, the second term is the spin-orbit coupling interaction, the third term denotes the ligand-field interaction, and the last term represents the Zeeman interaction. ζ and k are the spin-orbit coupling coefficient and the orbital reduction factor, respectively. V_i is the potential function which can be expressed as

$$\begin{aligned}V_i = \gamma_{00} Z_{00} + \gamma_{20} r_i^2 Z_{20}(\theta,\varphi_i) + \gamma_{40} r_i^4 Z_{40}(\theta_i,\varphi_i) \\ + \gamma_{43}^c r_i^4 Z_{43}^c(\theta_i,\varphi_i) + \gamma_{43}^s r_i^4 Z_{43}^s(\theta_i,\varphi_i),\end{aligned} \tag{3}$$

where r_i, θ_i and φ_i are the spherical coordinates of the i-th electron. Z_{lm}, Z_{lm}^c and Z_{lm}^s are the real spherical harmonics. γ_{l0}, γ_{lm}^c and γ_{lm}^s are associated with the local structure around a d^8 configuration ion by the relations

$$\begin{aligned}\gamma_{l0} &= -\frac{4\pi}{2l+1} \sum_{\tau=1}^{n} \frac{eq_\tau}{R_\tau^{l+1}} Z_{l0}(\theta_\tau,\varphi_\tau), \\ \gamma_{lm}^c &= -\frac{4\pi}{2l+1} \sum_{\tau=1}^{n} \frac{eq_\tau}{R_\tau^{l+1}} Z_{lm}^c(\theta_\tau,\varphi_\tau), \\ \gamma_{lm}^s &= -\frac{4\pi}{2l+1} \sum_{\tau=1}^{n} \frac{eq_\tau}{R_\tau^{l+1}} Z_{lm}^s(\theta_\tau,\varphi_\tau),\end{aligned} \tag{4}$$

where θ_τ and φ_τ are angular coordinates of the ligand, τ and q_τ represent the τ-th ligand ion and its effective charge, respectively, and R_τ denotes the metal-ligand distance.

The 45×45 complete energy matrices for a d^8 configuration ion corresponding to the perturbation Hamiltonian have been constructed by using the Slater wave function method and the calculating procedure. The matrix elements can be expressed as the functions of the Racah parameters B, C, the spin-orbit coupling coefficient ζ, the orbital reduction factor k, and the ligand-field parameters B_{20}, B_{40}, B_{43}^c and B_{43}^s. For the $Zn(BF_4)_2 \cdot 6H_2O{:}Ni^{2+}$ system, the Ni^{2+} ion is surrounded by six H_2O molecules and the local structure symmetry belongs to the D_{3d} symmetry [22]. In general, the z-axis is chosen along the three fold axis and the x-axis is chosen to be consistent with the projection of one of the impurity-ligand bond in x-y plane. Then, the ligand-field parameter B_{43}^s will vanish, and B_{20}, B_{40}, B_{43}^c can be expressed as [26]

$$\begin{aligned}B_{20} &= \frac{1}{2} \sum_\tau G_2(\tau)(3\cos^2\theta_\tau - 1), \\ B_{40} &= \frac{1}{8} \sum_\tau G_4(\tau)(35\cos^4\theta_\tau - 30\cos^2\theta_\tau + 3), \\ B_{43}^c &= \frac{\sqrt{35}}{4} \sum_\tau G_4(\tau)\sin^3\theta_\tau \cos\theta_\tau.\end{aligned} \tag{5}$$

According to the Van Vleck approximation [27], $G_2(\tau)$ and $G_4(\tau)$ can be expressed as

$$\begin{aligned}G_2(\tau) &= -eq_\tau \frac{\langle r^2\rangle}{R_\tau^3} = \frac{A_2}{R_\tau^3}, \\ G_4(\tau) &= -eq_\tau \frac{\langle r^4\rangle}{R_\tau^5} = \frac{A_4}{R_\tau^5},\end{aligned} \tag{6}$$

where

$$A_2 = -eq_\tau\langle r^2\rangle, \quad A_4 = -eq_\tau\langle r^4\rangle, \quad \frac{A_2}{A_4} = \frac{\langle r^2\rangle}{\langle r^4\rangle}. \tag{7}$$

The ratio $\langle r^2\rangle/\langle r^4\rangle = 0.141029$ is derived from the empirical radial wave function of Ni^{2+} in complexes [28]. A_4 is almost a constant for $[Ni(H_2O)_6]^{2+}$ coordination complex and its value can be obtained from the corresponding optical spectra. Then, A_2 can be determined by (7). Although no optical spectra of $Zn(BF_4)_2 \cdot 6H_2O{:}Ni^{2+}$ system has been observed, it is reasonable to apply the optical spectra of $NiSiF_6 \cdot 6H_2O$ in calculation since they have the similar crystal structure and the same type of ligand. Therefore, we obtain

$A_4 = 20.9$ a. u. from the optical spectra and the local structure of the $NiSiF_6 \cdot 6H_2O$ [29, 30]. The advantage of determining the value of A_4 is to reduce the number of adjustable parameters and make the choosing of parameters more reasonable. Thus, the ligand-field parameters B_{20}, B_{40}, B_{43}^c are only the functions of distortion parameters R_τ and θ_τ which are strongly depended on the external factors such as temperature, concentration and pressure.

2.2. EPR Parameters for a d^8 Configuration Ion

EPR spectra for a d^8 configuration ion in a trigonal ligand-field can be analyzed by the spin Hamiltonian [31]

$$\hat{H}_S = \mu_B g_\parallel H_z S_z + \mu_B g_\perp (H_x S_x + H_y S_y) + D\left[S_z^2 - \frac{1}{3}S(S+1)\right], \tag{8}$$

where D is the ZFS parameter. H_x, H_y and H_z represent the components of an external magnetic field along the x, y and z-axes, respectively. It is well known that the ground state $^3A_2$ is split into the singlet $|0\rangle$ and the doublet $|\pm 1\rangle$ in the trigonal ligand-field in the absence of an external magnetic field. From the spin Hamiltonian, the splitting energy levels in the ground state $^3A_2$ for a zero magnetic field can be given as follows

$$\begin{aligned} E(M_s = 0) &= -\frac{2}{3}D, \\ E(M_s = \pm 1) &= \frac{1}{3}D. \end{aligned} \tag{9}$$

Then, the ZFS energy ΔE in the ground state $^3A_2$ can be explicitly expressed as a function of the ZFS parameter D

$$\Delta E = E(M_s = \pm 1) - E(M_s = 0) = D. \tag{10}$$

By diagonalizing the 45×45 complete energy matrices, we can obtain all the crystal-field energy levels in the trigonal ligand-field with zero-magnetic field.

When considering the external magnetic field effect, the ground state $^3A_2$ will be further split by the actual Zeeman interaction

$$\hat{H}_{Zeeman} = \sum_i \mu_B (k\vec{l}_i + g_e \vec{s}_i) \cdot \vec{H}, \tag{11}$$

where k is the orbital reduction factor describing the covalence and overlap effects on the orbital angular momentum. g_e is the g-factor of the free electron ($g_e = 2.0023$). The energy levels of the ground state $^3A_2$ with a magnetic field including the parallel and perpendicular component of Zeeman term are given as follows.

For the magnetic field parallel to the C_3 axis, the splitting energy levels of the ground state can be expressed as

$$\begin{aligned} E_1 &= -\frac{2}{3}D, \\ E_2 &= \frac{1}{3}D - g_\parallel \mu_B H_z, \\ E_3 &= \frac{1}{3}D + g_\parallel \mu_B H_z. \end{aligned} \tag{12}$$

For the magnetic field perpendicular to the C_3 axis, the splitting energy levels of the ground state can be expressed as

$$\begin{aligned} E_1 &= \frac{1}{3}D, \\ E_2 &= -\frac{1}{6}D + \frac{1}{2}\sqrt{D^2 + 4g_\perp^2 \mu_B^2 H_\perp^2}, \\ E_3 &= -\frac{1}{6}D - \frac{1}{2}\sqrt{D^2 + 4g_\perp^2 \mu_B^2 H_\perp^2}. \end{aligned} \tag{13}$$

The anisotropic g-factors ($g_\parallel, g_\perp$) and ZFS parameter D for a d^8 configuration ion in a trigonal ligand-field can be deduced from (12), (13) and the eigenvalues of the 45×45 complete energy matrices.

3. Calculation and Discussion

3.1. Calculation of the Local Structures of $[Ni(H_2O)_6]^{2+}$ Coordination Complex at Different Temperatures and Concentrations

$Zn(BF_4)_2 \cdot 6H_2O$ crystal has a pseudo hexagonal structure. The Zn^{2+} ion is surrounded by six H_2O molecules, which make up an octahedral structure slightly distorted along the C_3 axis. The $[Zn(H_2O)_6]^{2+}$ octahedron site is at the center of another flattened octahedron formed by six $[BF_4]^{-1}$ tetrahedrons, which also forms an octahedral structure [21]. When doped into $Zn(BF_4)_2 \cdot 6H_2O$ crystal, the Ni^{2+} ions will substitute the Zn^{2+} ions at the octahedral sites and the point symmetry of the H_2O octahedron surrounding the Ni^{2+} ion is approximately D_{3d}. The local structure around the Ni^{2+} ion can be described by two parameters R and θ, which denote the Ni^{2+}-H_2O distance and the

Table 1. The EPR parameters D, $g_\parallel$ and $g_\perp$ as a function of the parameters R and θ at 4.2 K, 77 K and room temperature (RT for short) when 1% Ni^{2+} ions doped in $Zn(BF_4)_2 \cdot 6H_2O$ crystal.

T (K)		R (Å)	θ (°)	$g_\parallel$	$g_\perp$	$-D$ (cm^{-1})
4.2	Calc.	2.032	54.779	2.2301	2.2291	0.135
	Obsd.[a]			2.23±0.002	2.19±0.002	0.1350±0.0004
77	Calc.	2.033	54.796	2.2309	2.2295	0.19067
	Obsd.[a]			2.23±0.005	2.23±0.005	0.1908±0.0004
RT	Calc.	2.047	54.928	2.2351	2.2305	0.63147
	Obsd.[a]			2.22±0.005	2.22±0.005	0.6314±0.0030

[a] Spectra data obtained from [22].

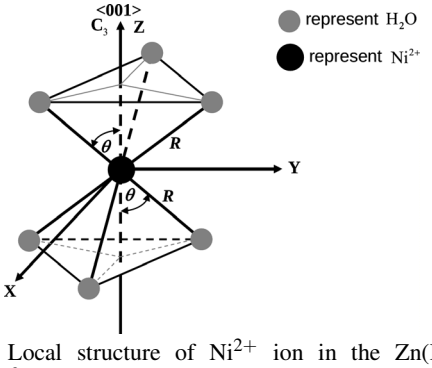

Fig. 1. Local structure of Ni^{2+} ion in the $Zn(BF_4)_2 \cdot 6H_2O$:Ni^{2+} system.

angle between Ni^{2+}-H_2O bond and C_3 axis, as shown in Figure 1.

According to Curie et al.'s covalence theory [32], the Racah parameters B, C and spin-orbit coupling coefficient ζ can be reasonably expressed as

$$B = N^4 B_0, \quad C = N^4 C_0, \quad \zeta = N^2 \zeta_0, \tag{14}$$

where N is the average covalence factor, $B_0 = 1084\,cm^{-1}$, $C_0 = 4831\,cm^{-1}$, $\zeta_0 = 649\,cm^{-1}$ are given for free Ni^{2+} ion [33]. The covalence factor $N = 0.965$ can be obtained from the optical spectra of $NiSiF_6 \cdot 6H_2O$ crystal [29]. Then, $k \approx N^2$ can also be obtained. The EPR parameters for 4.2 K, 77 K and room temperature when 1% Ni^{2+} impurities doped in $Zn(BF_4)_2 \cdot 6H_2O$ crystal have been measured by Krygin et al. [22]. By diagonalizing the complete energy matrices, the local structure parameters R and θ of $[Ni(H_2O)_6]^{2+}$ coordination complex at 4.2 K, 77 K and room temperature when 1% Ni^{2+} doped in $Zn(BF_4)_2 \cdot 6H_2O$ crystal can be determined by simulating the optical and corresponding EPR spectra. Quantitative calculated results are listed in Tables 1 and 2. As shown in Tables 1 and 2, the calculated values agree well with the experimental values. Table 1 depicts that the local structure around the octahedral Ni^{2+} ion has an expansion tendency with increasing temperature. It can be seen that $R = 2.032$ Å for 4.2 K and $R = 2.033$ Å for 77 K, suggesting that R is almost changeless in the low temperature range.

Table 2. The observed and calculated optical spectra of $[Ni(H_2O)_6]^{2+}$ in $NiSiF_6 \cdot 6H_2O$ crystal at 4.2 K, 77 K and room temperature (all units in cm^{-1}).

Transition	4.2 K		77 K		Room temp.	
	Obsd.[a]	Calc.	Obsd.[a]	Calc.	Obsd.[a]	Calc.
$^3A_2(F) \rightarrow {}^3T_2(F)$	9150	9150	9120	8800	9124	8794
		9161		9140		8843
$^3T_1(F)$	15400	15129	15290	15093	14800	14618
		15149		15122		14707
$^1E(D)$		15363		15362		15345
$^1T_2(D)$		24083		24054		23677
		24104		24082		23769
$^1A(G)$	24450	24763		24755		24643
$^3T_1(P)$	26100	26401	26000	26351		25774
		26456		26429		26014
$^1T_1(G)$		28809	29070	28783	28820	28453
		28820		28799		28502

[a] Spectra data obtained from [29].

Table 3. The EPR parameters D, $g_\parallel$ and $g_\perp$ as a function of the parameters R and θ at 4.2 K, 77 K and room temperature (RT for short) when 1.5% (2.7% for 4.2 K) Ni^{2+} ions doped in $Zn(BF_4)_2 \cdot 6H_2O$ crystal.

T (K)		R (Å)	θ (°)	$g_\parallel$	$g_\perp$	$-D$ (cm^{-1})
4.2	Calc.	2.032	54.777	2.2378	2.2368	0.12905
	Obsd.[a]			2.229±0.006	2.261±0.025	0.1291±0.0008
77	Calc.	2.033	54.796	2.2387	2.2372	0.18973
	Obsd.[a]			2.27±0.006	2.263±0.028	0.1898±0.0009
RT	Calc.	2.047	54.925	2.2486	2.2438	0.62018
	Obsd.[a]			2.24±0.012	2.25±0.012	0.620±0.0040

[a] Spectra data obtained from [21].

Table 4. The EPR parameters D, $g_\parallel$ and $g_\perp$ as a function of the parameters R and θ at 4.2 K, 77 K and room temperature (RT for short) when 100% Ni^{2+} ions doped in $Zn(BF_4)_2 \cdot 6H_2O$ crystal.

T (K)		R (Å)	θ (°)	$g_\parallel$	$g_\perp$	$-D$ (cm^{-1})
4.2	Calc.	2.032	54.775	2.2507	2.2497	0.124
	Obsd.[a]			2.27±0.04		0.1240±0.0050
77	Calc.	2.033	54.79	2.2515	2.2501	0.1703
	Obsd.[a]			2.254±0.020	2.366±0.020	0.1703±0.0010
RT	Calc.	2.047	54.899	2.2616	2.2572	0.5371
	Obsd.[a]			2.311±0.025	2.226±0.025	0.537±0.0040

[a] Spectra data obtained from [21].

The EPR parameters for different temperatures when 1.5% and 100% Ni^{2+} impurities doped in $Zn(BF_4)_2 \cdot 6H_2O$ crystal have been studied by Sano

et al. [21]. As mentioned by many authors [34–36], the ZFS parameter D strongly depends on θ. Therefore, in order to study the behaviour of θ under different concentrations, R is fixed for the certain temperature. Then, the local angle under different concentrations can be obtained by simulating EPR spectra and the calculated results are shown in Tables 3 and 4, respectively. Comparing with Tables 1, 3 and 4, we can see that θ decreases when the Ni^{2+} molar concentration increases from 1% to 100%. This may be ascribed to that the ionic radius of Ni^{2+} is smaller than that of Zn^{2+}, and when Ni^{2+} ions replace the Zn^{2+} ions in $Zn(BF_4)_2 \cdot 6H_2O$ crystal, the Ni^{2+} ions will pull the H_2O ligands inwards.

3.2. *Calculation of the Local Structures of $[Ni(H_2O)_6]^{2+}$ Coordination Complex at Different Pressures*

The observed hydrostatic pressure dependence of D at 77 K, i. e. $D = (-0.196 + 0.06P)$ cm^{-1} and the value $D = (-0.1908 \pm 0.0004)$ cm^{-1} have been obtained by Krygin et al. [22], from which we can get $P \approx 0.089$ kbar. The local structure parameters $R = 2.033$Å and $\theta = 54.796°$ at $P \approx 0.089$ kbar are given in Tables 1 and 3. As previously mentioned, R is almost changeless in the low temperature range. Therefore, in order to discern the relationship between θ and P, $R = 2.033$ Å is considered as a constant. The relationship between the EPR parameters and the local structure parameter θ in the pressure range 0 kbar $\leq P \leq 4$ kbar at 77 K is shown in Table 5. The pressure dependence of the local structure parameter θ and anisotropic g-factors ($g_\parallel$ and $g_\perp$) are depicted in Figure 2 and the relationship between D and Δg ($g_\parallel$-$g_\perp$) is shown in Figure 3.

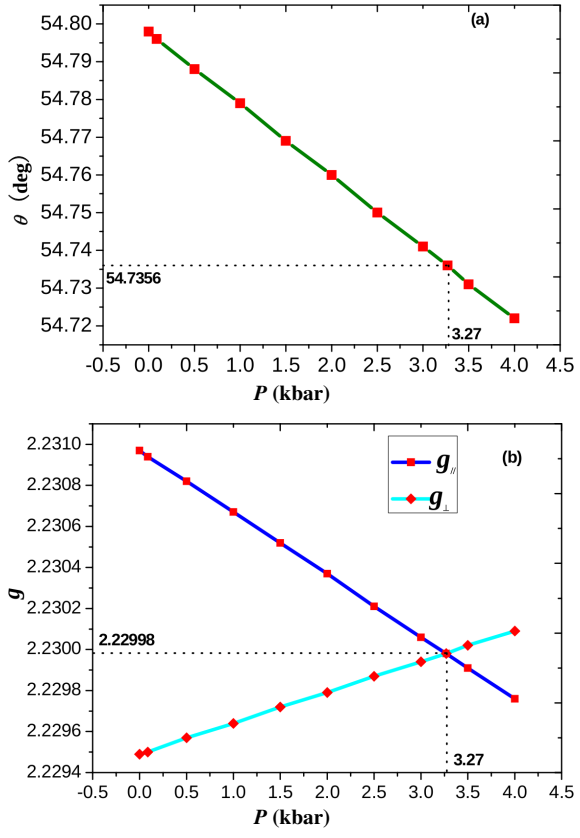

Fig. 2. Pressure dependence of (a) local structure parameter θ and (b) g-factors ($g_\parallel$ and $g_\perp$).

Table 5. The EPR parameters D, $g_\parallel$ and $g_\perp$ in the pressure range 0 kbar $\leq P \leq 4$ kbar at 77 K for Ni^{2+} doped $Zn(BF_4)_2 \cdot 6H_2O$ crystal as a function of θ. (The values of $D_{Expt.}$ and D_p are obtained from the experimental formula $D = (-0.196 + 0.06P)$ cm^{-1} [22] and from the 45×45 complete energy matrices, respectively.)

P (kbar)	$-D_{Expt.}$ (cm^{-1})	$g_\parallel$	$g_\perp$	Δg	θ (°)	$-D_p$ (cm^{-1})
0	0.196	2.23097	2.22949	0.00148	54.798	0.196
0.087	0.1908	2.23094	2.2295	0.00144	54.796	0.1907
0.5	0.166	2.23082	2.22957	0.00125	54.788	0.1659
1.0	0.136	2.23067	2.22964	0.00103	54.779	0.1361
1.5	0.106	2.23052	2.22972	0.00080	54.769	0.1060
2.0	0.076	2.23037	2.22980	0.00057	54.76	0.0761
2.5	0.046	2.23021	2.22987	0.00034	54.75	0.0459
3.0	0.016	2.23006	2.22994	0.00012	54.741	0.0160
3.27	0	2.22998	2.22998	0	54.7356	0
3.5	−0.014	2.22991	2.23002	−0.00011	54.731	−0.0139
4.0	−0.044	2.22976	2.23009	−0.00033	54.722	−0.0441

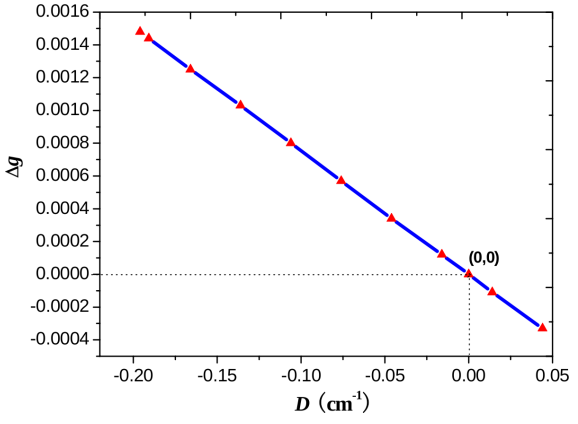

Fig. 3. The relationship between ZFS parameter D and Δg.

As depicted in Figure 2, θ diminishes along with the increasing pressure and the relation between them

is approximately linear. Moreover, Figure 2 indicates that $g_\parallel$ decreases while $g_\perp$ increases with increasing pressure. Figure 3 shows that D and Δg reverse sign in a correlated way, i. e. for $D < 0$, $\Delta g > 0$, whereas for $D > 0$, $\Delta g < 0$. It's worth pointing that when the pressure reaches to 3.27 kbar, $D = 0$s and $g_\parallel = g_\perp = 2.22998$. Meanwhile, the angle becomes 54.7356°, which is the angle when the ligand octahedron is a cubic symmetry.

4. Conclusion

The local structures for Ni^{2+} ions in $Zn(BF_4)_2 \cdot 6H_2O$:Ni^{2+} system at different temperatures (4.2 K, 77 K, and room temperature), molar concentrations (1%, 1.5%, and 100%), and pressures (0 kbar $\leq P \leq$ 4 kbar) are determined by diagonalizing the 45×45 complete energy matrices. From the above studies, we have the following conclusions:

(i) The local structures around the octahedral Ni^{2+} ion have expansion distortions with the increasing temperature.

(ii) The calculated results show that θ becomes smaller with increasing concentration of Ni^{2+} ions doped in $Zn(BF_4)_2 \cdot 6H_2O$ crystal. We attribute it to that the ionic radius of Ni^{2+} is smaller than that of Zn^{2+} and the Ni^{2+} ion will pull the H_2O ligands inwards.

(iii) The structure parameter θ will decrease as the pressure increases and the relation between them are approximately linear. Meanwhile, the results show that $g_\parallel$ decreases while $g_\perp$ increases with increasing pressure and D and Δg reverse sign in a correlated way, i. e. for $D < 0$, $\Delta g > 0$, whereas for $D > 0$, $\Delta g < 0$. Of course, careful experimental investigations, especially the optical spectra experiments, are required in order to clarify the local structure for Ni^{2+} ions in $Zn(BF_4)_2 \cdot 6H_2O$:Ni^{2+} system in detail.

Acknowledgements

The authors are grateful to the National Natural Science Foundation of China (No. 10774103) and the Doctoral Education Fund of Education Ministry of China (No. 20050610011).

[1] K. Ragavendran, A. Nakkiran, P. Kalyani, A. Veluchamy, and R. Jagannathan, Chem. Phys. Lett. **456**, 110 (2008).
[2] B. S. Reddy, N. O. Gopal, K. V. Narasimhulu, Ch. L. Raju, J. L. Rao, and B. C. V. Reddy, J. Mol. Struct. **751**, 161 (2005).
[3] O. Pilla, P. T. C. Freire, and V. Lemos, Phys. Rev. B **52**, 177 (1995).
[4] J. Pisarska, W. A. Pisarski, G. Dominiak, and W. R. Romanowski, J. Mol. Struct. **792 – 793**, 201 (2006).
[5] D. J. Keeble and M. Loyo-Menoyo, Phys. Rev. B **71**, 224111 (2005).
[6] H. Akai and M. Ogura, Phys. Rev. Lett. **97**, 026401 (2006).
[7] M. Syed and A. Siahmakoun, Opt. Mater. **27**, 1639 (2005).
[8] P. Srivastava, O. N. Srivastava, H. K. Singh, and P. K. Siwach, J. Alloys Compd. **459**, 61 (2008).
[9] M. Grinberg, A. Sikorska, A. Sliwinski, and J. Barzowska, Phys. Rev. B **67**, 045113 (2003).
[10] Y. Q. Jiang, L. E. Halliburton, M. Roth, M. Tseitlin, and N. Angert, Physica B **400**, 190 (2007).
[11] D. M. Murphy, R. D. Farley, J. Marshall, and D. J. Willock, Chem. Phys. Lett. **391**, 1 (2004).
[12] S. Schweizer and J. M. Spaeth, J. Phys. Chem. Solids **58**, 859 (1997).
[13] M. Warkentin, F. Bridges, S. A. Carter, and M. Anderson, Phys. Rev. B **75**, 075301 (2007).
[14] E. Gaudry, D. Cabaret, C. Brouder, I. Letard, A. Rogalev, F. Wilhlem, N. Jaouen, and P. Sainctavit, Phys. Rev. B **76**, 094110 (2007).
[15] J. Chen, H. Zhang, I. V. Tomov, X. L. Ding, and P. M. Rentzepis, Chem. Phys. Lett. **437**, 50 (2007).
[16] S. A. Basun, V. E. Bursian, D. R. Evans, A. A. Kaplyanskii, A. G. Razdobarin, and L. S. Sochava, Phys. Rev. Lett. **100**, 057602 (2008).
[17] G. Völkel and K. A. Müller, Phys. Rev. B **76**, 094105 (2007).
[18] S. Moribe, T. Ikoma, K. Akiyama, Q. W. Zhang, F. Saito, and S. T. Kubota, Chem. Phys. Lett. **436**, 373 (2007).
[19] G. Mallia and N. M. Harrison, Phys. Rev. B **75**, 165201 (2007).
[20] S. Isber, M. Tabbal, T. Christidis, S. Charar, F. Terki, and M. Ishii, Phys. Rev. B **71**, 014405 (2005).
[21] W. Sano, J. B. Domiciano, and J. A. Ochi, Phys. Rev. B **50**, 2958 (1994).
[22] I. M. Krygin, A. A. Prokhorov, G. N. Neilo, and A. D. Prokhorov, Phys. Solid State **43**, 2147 (2001).
[23] W. Sano, S. Isotani, J. A. Ochi, and J. C. Sartorelli, J. Phys. Soc. Jpn. **46**, 26 (1979).
[24] J. B. Domiciano, W. Sano, K. R. Juraitis, and S. Isotani, J. Phys. Soc. Jpn. **48**, 1449 (1980).
[25] W. L. Feng, W. C. Zheng, X. X. Wu, and H. G. Liu, Physica B **387**, 52 (2007).
[26] D. J. Newman and W. Urban, Adv. Phys. **24**, 793 (1975).
[27] J. H. Van Vleck, Phys. Rev. **41**, 208 (1932).

[28] M. G. Zhao, M. L. Du, and G. Y. Sen, J. Phys. C: Solid State Phys. **20**, 5557 (1987).
[29] M. H. L. Pryce, G. Agnetta, T. Garofano, M. B. Paima-Vittorelli, and M. U. Palma, Phil. Mag. **10**, 477 (1964).
[30] S. Ray, A. Zalkin, and D. H. Temleton, Acta. Crystallogr. B **29**, 2741 (1973).
[31] A. Abragam and B. Bleaney, Electron Pramagnetic Resonance of Transition Ions, Oxford University Press, London 1970.
[32] D. Curie, C. Barthon, and B. Canny, J. Chem. Phys. **61**, 3048 (1974).
[33] J. S. Griffith, The Theory of Transition-Metal Ions, Cambridge University Press, London 1964, p. 487.
[34] Z. M. Li and W. L. Shuen, Physica B **222**, 238 (1996).
[35] T. How and I. Svare, Phys. Scripta **9**, 40 (1974).
[36] A. Krupska and M. Krupski, Acta Phys. Pol. A **103**, 453 (2003).